J Electroceram (2009) 23:356–360
DOI 10.1007/s10832-008-9466-6

Electrical and optical studies of transparent conducting ZnO:Al thin films by magnetron dc sputtering

Vinh Ai Dao · Tran Le · Tuan Tran · Huu Chi Nguyen · Kyunghae Kim · Jaehyeong Lee · Sungwook Jung · N. Lakshminarayan · Junsin Yi

Received: 31 May 2007 / Accepted: 21 February 2008 / Published online: 13 March 2008
© Springer Science + Business Media, LLC 2008

Abstract Transparent conducting aluminium-doped Zinc oxide (ZnO:Al) films have been deposited on glass substrates by magnetron dc sputtering using a ceramic target (ZnO with 2 wt% Al_2O_3). The dependence of the electrical and optical properties of these films on substrate temperature, sputtering pressure of Ar and location of substrates were investigated in detail. Target is perpendicular with substrate and we controlled the distance ‘x’ of target and substrate. Optimized films with resistivity of 3.7×10^{-4} Ω cm, an average transmission in the visible range (300–800 nm) of greater than 85% and the reflectance in the infrared range being greater than 85% have been formed. Substrate temperature, distance ‘x’, and working pressure are optimized for lower resistivity and high concentration of carriers.

Keywords Transparent conductive oxide films · Energetic oxygen atoms · ZnO:Al

V. A. Dao · K. Kim · S. Jung · N. Lakshminarayan · J. Yi (✉)
Information Communication Device Lab,
Sungkyunkwan University,
Suwon, South Korea
e-mail: yi@yurim.skku.ac.kr

T. Le · T. Tran · H. C. Nguyen
Ho Chi Minh City University of Natural Sciences,
Ho Chi Minh City, Vietnam

J. Lee
Electronics and Information Engineering,
Kunsan National University,
Gunsan, South Korea

N. Lakshminarayan
Department of Physics, Madras Christian College,
Chennai 600059, India

1 Introduction

The n-type Al-doped semiconductive ZnO thin films have high energy band gap. It has wide applications as transparent electrode in solar cells, displays, or low emissivity coatings. To compare with ITO thin films, it is clearly that ZnO is a low cost material. Hence, much work on conductive ZnO thin films [1, 2] has been reported, recently.

Compared to other thin-film deposition methods such as evaporation, chemical vapor deposition (CVD) or spray pyrolysis, magnetron sputtering is characterized by the following advantages [3]:

- low substrate temperatures (down to room temperature)
- good adhesion of films on substrates
- high deposition rates (up to 12 μm/min)
- very good thickness uniformity and high density of the films
- good controllability and long-term stability of the process
- alloys and compounds of materials with very different vapor pressures can be sputtered easily
- by reactive sputtering in rare/reactive gas mixtures many compounds can be deposited from elemental (metallic) targets
- relatively cheap deposition method
- scalability to large areas (up to 3–6 m^2).

The problem in magnetron sputtering techniques has been the unwanted bombardment of the growing thin films by negative ions and high energy neutral atoms. This bombardment has been found consequential to high resistivity thin films [1, 2]. It has been shown [4] that the main reason for negative ions was the surface ionization of

the target surface. The contribution of negative ions current is mainly from the erosion area because of its higher temperature.

2 Experimental

Glass substrates were dipped in 5% dilute HF in 5 min, followed by in acetone in 5 min and rinsed in DI water in 5 min. The substrate size is 2×7 cm^2 and substrate thickness is 2 mm. The glass substrates were dried at 150 °C to remove of remaining vapor of water on its surface.

The Al-doped conductive ZnO thin films were prepared by the sputtering of a ZnO ceramic target doped with 2 wt% Al_2O_3 and 7×7 cm^2 in dimensions. The working pressure of argon (99.5%) was varied from 9 to 1 mTorr, with a sputtering power of 60 W, at a sputtering current of 0.2 A. A pre-sputter etching of the target was carried out to expose a clean surface at the target. The glass substrate was attached to the substrate heater, and it was located perpendicular to the target as showing in Fig. 1. The rate of deposition is approximately from 20 to 30 nm/min. The temperature of the substrate was varied from 120 to 280 °C.

The crystal structure was determined using 0.15418 nm line of the X-ray diffractometer. The optical transmission spectra were measured in the wavelength range from 300 to 1,100 nm. The optical reflectance spectra were measured in the wavelength range from 660 to 25,000 nm. The thickness of thin films was determined by Swanepoel's method [5]. Sheet resistances were measured by four point probe. The concentration of carriers was determined from the plasma wavelength λ_p [8, 11, 12].

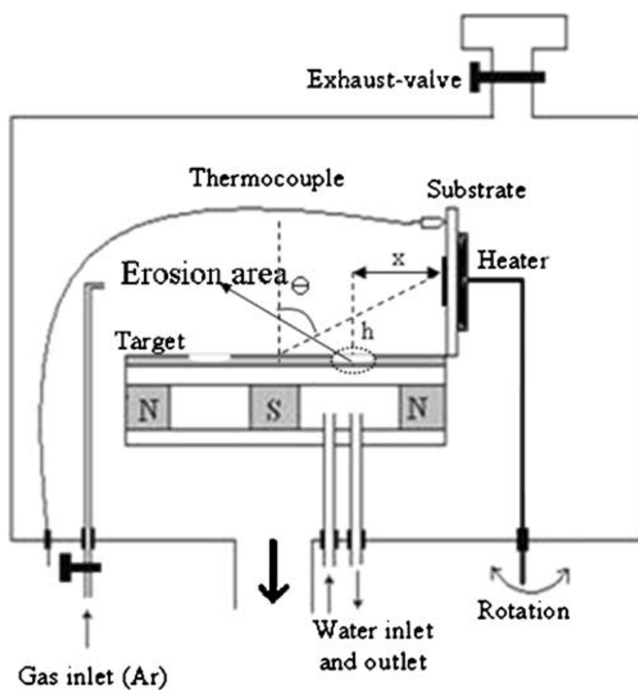

Fig. 1 Schematic diagram of sputtering system

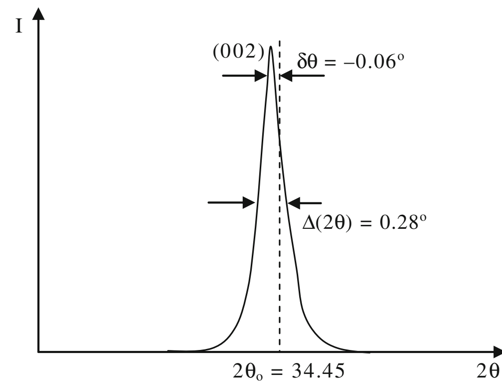

Fig. 2 X-ray diffraction of ZnO:Al thin films preparation at 1 mTorr working pressure, 160 °C substrate temperature

3 Results and discussions

Figure 1 shows the sputter diagram with target, substrate, exhaust, and gas line. Conventionally, target and substrate are parallel in sputter chamber. Erosion areas are caused from strong magnetic field on the target. Two erosion areas are center of magnetic field on north and south poles. In conventional sputter chamber, ZnO:Al thin film on substrate has a poor quality due to strong bombardment of negative ions. To overcome the above disadvantages, the substrate and target were arranged perpendicular to each other, for which the distribution of a depositing rate is followed by $f(\theta) = \cos(\theta) + a \times \cos^3(\theta) (a = -0.8)$ that mean the maximum of sputtering direction varies from 30° to 40° [6], and then temperature T_s, work pressure P_{Ar}, distance 'x' were adjusted to obtain optimized deposition conditions in Fig. 1. Substrate can move arranged perpendicular with target. The "x" means distance of center of erosion area to substrate in Fig. 1. The "h" means height of target to center of sample on substrate.

3.1 Crystal structure characterization

Figure 2 showed only the (002) XRD peak with high intensity in the ZnO:Al thin film, indicating that they had *c*-axis normal to the substrate. Stress of thin films was determined using the relation of θ and $\delta\theta$ in Eq. 1:

$$\sigma_f = \frac{Y}{2\nu} \frac{\delta\theta}{\tan\theta} \quad (1)$$

where σ_f is stress of thin films, Y is the Young modulus; υ is the Poisson coefficient; $\delta\theta = \theta - \theta_o$, where θ is the diffraction angle from XRD of thin films; θ_o is the diffraction angle that is taken from XRD data of bulk

material. Scherrer's formula was used to estimate grain size of ZnO thin films:

$$b = \frac{0.9\lambda}{\Delta(2\theta)\cos(\theta)} \quad (2)$$

where b means grain size of film, λ (=0.15418 nm) means the wavelength of X-ray; $\Delta(2\theta)$ is the half width of the (002) diffraction line. θ is the Bragg's diffraction.

Figure 3(a) shows grain size of ZnO:Al thin film and $\delta\theta$ in XRD data as a function of 'x' in 120 °C substrate temperature and 3 mTorr working pressure. Stress is dependent of $\delta\theta$ and stress of thin film is not only dependent of 'x' but also pressure in chamber in Fig. 3(a) and (b).

The grain size varied in the short range and is highest in value of 'x' from 2.5 to 3 cm. These results indicate that the ZnO thin films are bombarded by the high energy ions in the 2.5–3 cm distance. Figure 3(b) shows largest grain size in low pressure as 1 mTorr. This result indicates that bombarding on substrate is the highest at the lowest pressure in Fig. 3(b). However, there are small variations in the electrical properties, because the slight variations in grain size do not lead to pronounced grain boundary scattering effects.

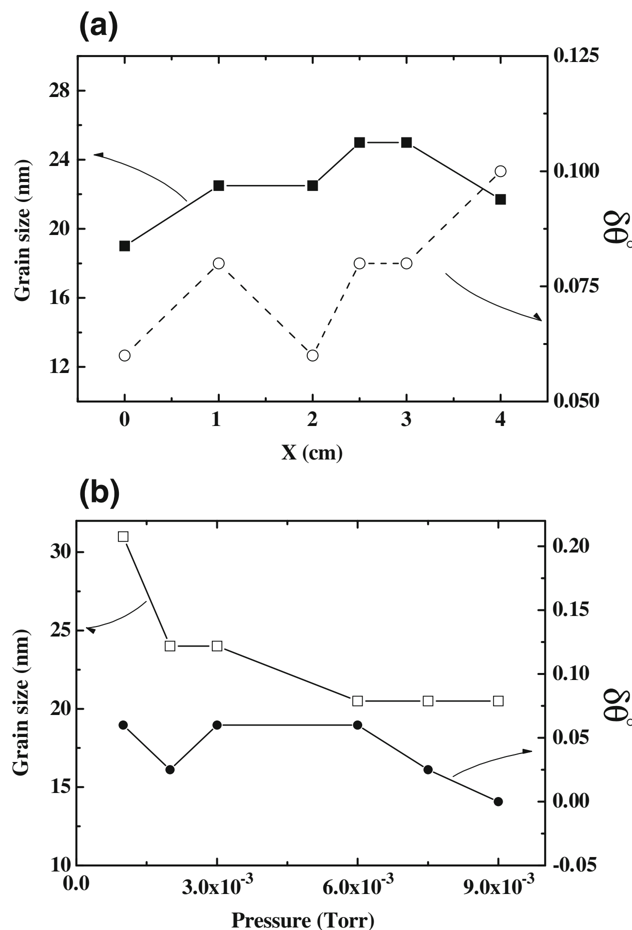

Fig. 3 (**a**) Grain size and shift angle versus distance (120 °C substrate temperature, 3 mTorr working pressure). (**b**) Grain size and shift angle versus pressure (substrate temperature, 2.5 cm distance 'x')

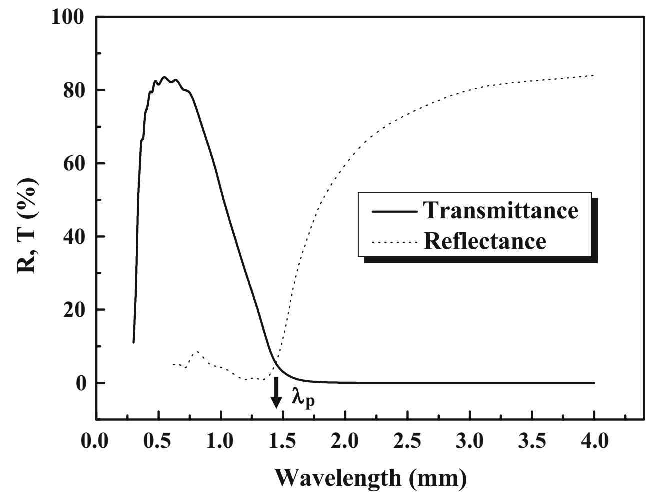

Fig. 4 Reflectance and transmittance for ZnO:Al thin films (160 °C substrate temperature, 3 mTorr working pressure, 2.5 cm distance 'x')

3.2 Optical and electrical properties

The transmission and reflectance spectrum of ZnO thin films is shown in Fig. 4. ZnO:Al thin film was deposited in 160 °C substrate temperature, 3 mTorr working pressure, and 2.5 cm distance.

The average transmission in the visible range (300–800 nm) is greater than 85% and the reflection in the infrared range is greater than 85%.

The Drude theory describes the free electron contribution to the dielectric function by [7]:

$$\varepsilon_1^{\mathrm{Drude}}(\omega) = \varepsilon_\infty - \left[\omega_N^2/\left(\omega^2+\gamma^2\right)\right] \quad (3)$$

$$\varepsilon_2^{\mathrm{Drude}}(\omega) = (\gamma/\omega)\left[\omega_N^2/\left(\omega^2+\gamma^2\right)\right] \quad (4)$$

where ε_∞ is the dielectric constant extrapolated towards high energy ($\varepsilon_\infty \approx 4.5$) [9], and $\hbar\gamma$ is a relaxation energy which may be taken as energy-independent for qualitative analyses. The concentration of carriers of n_e and the effective conduction-band mass of the electrons m_c^* determine ω_N through:

$$\omega_N^2 = n_e e^2 / \varepsilon_0 m_c^* \quad (5)$$

where ε_0=8.854×10^{-12} As/Vm is the permittivity of free space. The energy at which ε=0, the longitudinal plasma energy $\hbar\omega_\mathrm{p}$ is approximately related to $\hbar\omega_N$ by:

$$\omega_\mathrm{p}^2 = \left(\omega_N^2/\varepsilon_\infty\right) - \gamma^2. \quad (6)$$

Frequency of plasma ω_p can be shift to high energy region of 0.7–1 eV because of high concentration of free electrons with ZnO or ITO. The most results from experiment is that

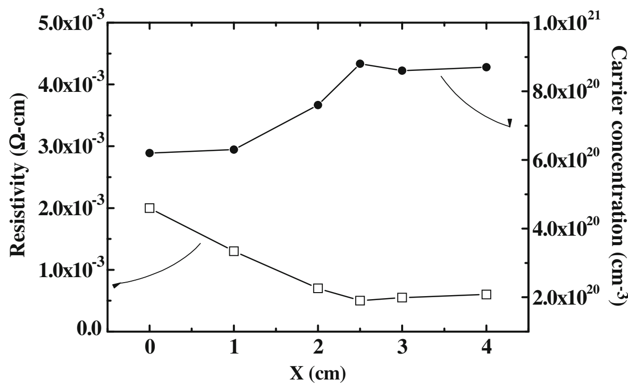

Fig. 5 Resistivity and concentration of carriers of versus distance

the values of $\overline{h}\gamma$ is around of 0.05–0.2 and $\overline{h}\omega_{\rm p}$ is around of 1 eV [7]. Therefore, it may assume $\omega_{\rm p}^2 >> \gamma^2$, and hence:

$$\omega_{\rm p}^2 \approx \frac{\omega_N^2}{\varepsilon_\infty}. \tag{7}$$

From Eqs. 5 and 7, the concentration of carriers was determined by following equation:

$$n_e \approx \frac{\omega_{\rm p}^2 \times \varepsilon_\infty \times \varepsilon_0 \times m_c^*}{e^2} \tag{8}$$

where $\omega_{\rm p} = \frac{2\pi c}{\lambda_{\rm p}}$, $\lambda_{\rm p}$ is resonant wavelength of the plasma. It is determined by intersection of transmission and reflectance spectrum.

Figure 5 shows the variations of the resistivity and the concentration of carriers with distance ‘x’. In this case, the substrate temperature, the chamber pressure, and the sputtering power are maintained constant at 120 °C, 3 mTorr and 60 W, respectively. We notice that the concentration of carriers rapidly increased for ‘x’ variation from x=0 cm to x=2.5 cm. This may be due to the bombardment of the substrate by positive ions. The value of the resistivity is 4.3× 10^{-4} Ωcm, with x=2.5 cm. The concentration of carriers shows a slight decrease for ‘x’ values of over 2.5 cm.

Figure 6 shows the variations of resistivity and concentration of carriers for different substrate temperatures from 120 to 280 °C at 3 mTorr pressure and 2.5 cm as ‘x’ distance. The lowest of resistivity and the highest concentration of carriers is seen to be got at 160 °C as substrate temperature in Fig. 6. As the temperature of the substrate increased, the resistivity increased because of reducing of concentration of carriers.

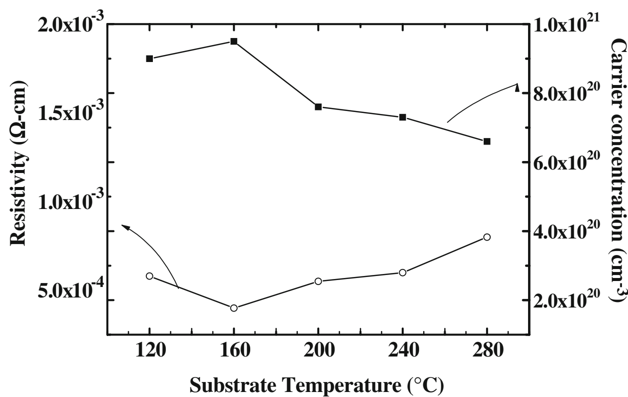

Fig. 6 Resistivity and concentration of carriers versus temperature

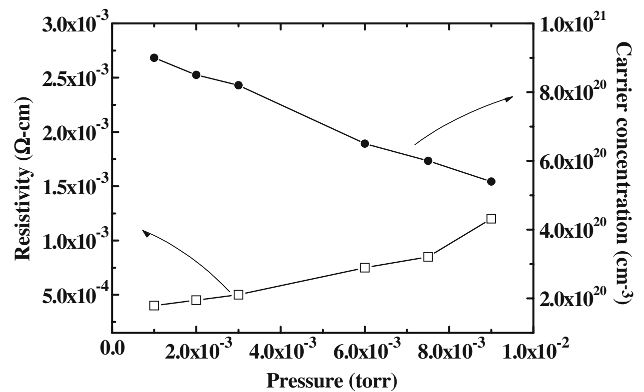

Fig. 7 Resistivity and concentration of carriers versus pressure

The reason for the reduction in the concentration of carriers may be explained as follows: Hong et al. [10] reported that as the temperature of the substrate increased due to the ion bombardment during films deposition, Zn content decreased and Al content increased in the films. As is well known, higher levels of Al incorporation lead to interstitial incorporation of Al in the form of Al_2O_3 giving rise to greater electron scattering [14]. The aluminum atoms may also segregate to the grain boundaries in the form of Al_2O_3 that will increase the grain boundary barrier [15]. Therefore, the concentration of carriers decrease as Zn is substituted by aluminum due to more scattering and grain boundary effects.

Figure 7 shows the variations of concentration of carriers versus the working pressure $P_{\rm Ar}$, with 160 °C substrate temperature, and 2.5 cm distance as ‘x’. In this case, as the working pressures increased so the scattering of O^- and the working gas increase. Hence, the resistivity increased because defects of O^- increased. Therefore, the optimal conditions for preparing suitable ZnO:Al thin films were in 1 mTorr pressure of Ar, 160 °C substrate temperature, and 2.5 cm ‘x’ distance.

4 Conclusions

Optimised ZnO:Al thin films were prepared using magnetron dc sputtering by placing the substrate perpendicular to the target, at a ‘x’ distance of 2.5 cm, substrate temperature of 160 °C and working pressure of 1 mTorr. This resulted in films with the lowest resistivity of 3.7×10^{-4} Ωcm and a larger concentration of carriers of 9×10^{20} cm^{-3}, with an average transmission in the visible range (300–800 nm) of greater than 85% and the reflectance in the infrared range

being greater than 85%. The values reported here are seen to be better than the previous reports. The main reason that may be attributed to the better results could be the attempt in this investigation to reduce the bombardment by negative ions that were emitted from target surface. The resistivity values agree with earlier reports [13] where the negative ion bombardment had been reduced by placing the substrate at the center of the target. The method used in this investigation may be adapted easily for mass production.

Acknowledgement This research was supported by the Ministry of Information and Communication (MIC), Korea, under the IT Foreign Specialist Inviting Program (ITFSIP) supervised by the Institute of Information Technology Advancement (IITA).

References

1. G.A. Hirata, J. McKittrick, J. Siqueiros, O.A. Lopez, T. Cheeks, O. Contreras, J.Y. Yi, J. Vac. Sci. Technol. A **14**(3), 791 (1996)May/June
2. K. Tominaga, S. Iwamura, Y. Shintani, O. Tada, Jpn. J. Appl. Phys **21**, 688–695 (1982)
3. K. Ellmer, J. Phys. D Appl. Phys **33**, R17–R32 (2000)
4. T. Le, H.C. Nguyen, T. Tran, J. Sci. Tech. Dep. **9**(8), Vietnam National University Ho Chi Minh City, Oct 2003
5. R. Swanepoel, J. Phys. E Sci. Instrum **16**, 1214–1222 (1983)
6. Y.E. Lee, S.G. Kim, Y.J. Kim, H.J. Kim, J. Vac. Sci. Technol. A **15**(3), 1194–1199 (1997)May/June
7. I. Hamberg, C.G. Granqvist, J. Appl. Phys **60**, R123 (1986)
8. H. Kim, A. Piqueù, J.S. Horwitz, H. Murata, Z.H. Kafafi, C.M. Gilmore, D.B. Chrisey, Thin Solid Films **377–378**, 798–802 (2000)
9. Y. Qu, T.A. Gessert, K. Ramathan, R.G. Dhere, R. Noufi, T.J. Coutts, J. Vac. Sci. Technol. A **11**(4), 996–1000 (1993)July/August
10. R.J. Hong, Jiang, B. Szyszka, V. Sittinger, A. Pflug, Appl. Surf. Sci **207**, 341–350 (2003)
11. D.H. Zhang, T.L. Yang, Q.P. Wang, D.J. Zhang, Mater. Chem. Phys **68**, 233–238 (2001)
12. T.J. Coutts, D.L. Young, X. Li, MRS Bull. **25**, 58–65 (2000)
13. T. Minami, T. Yamamoto, T. Miyata, Thin Solid Films **366**, 63–68 (2000)
14. J.F. Chang, M.H. Hon, Thin Solid Films **386**, 76 (2001)
15. T. Minami, H. Sato, K. Ohashi, T. Tomofuji, S. Takana, J. Cryst. Growth **117**, 370 (1992)